Revista Brasileira de Farmacognosia 26 (2016) 147–160

Brazilian Journal of Pharmacognosy
REVISTA BRASILEIRA DE FARMACOGNOSIA
www.elsevier.com/locate/bjp

Original Article

Structure and histochemistry of medicinal species of *Solanum*

Laudineia J. Matias[a], Maria O. Mercadante-Simões[a,*], Vanessa A. Royo[b], Leonardo M. Ribeiro[c], Ariadna C. Santos[a], Jaciara M.S. Fonseca[b]

[a] *Laboratório de Anatomia Vegetal, Departamento de Biologia Geral, Universidade Estadual de Montes Claros, Campus Pr. Darcy Ribeiro, Montes Claros, MG, Brazil*
[b] *Laboratório de Produtos Naturais, Departamento de Biologia Geral, Universidade Estadual de Montes Claros, Campus Pr. Darcy Ribeiro, Montes Claros, MG, Brazil*
[c] *Laboratório de Micropropagação, Departamento de Biologia Geral, Universidade Estadual de Montes Claros, Campus Pr. Darcy Ribeiro, Montes Claros, MG, Brazil*

ARTICLE INFO

Article history:
Received 12 June 2015
Accepted 4 November 2015
Available online 11 December 2015

Keywords:
Environmental conservation
Herbal medicine
Plant drug
Pharmacognosy
Phytochemical
Traditional medicine

ABSTRACT

Studies on native medicinal plants strengthen initiatives to preserve the environments where those species naturally occur, many of them already strongly menaced even before their potential to humankind is known. Root and stem barks, leaves, and pericarps samples of *Solanum agrarium* Sendtn., *S. lycocarpum* A. St.-Hil., *S. palinacanthum* Dunal, *S. paniculatum* L., and *S. stipulaceum Roem.* & Schult., species that occur in the Cerrado (Brazililan savanna) were processed according to common light microscopy techniques for structural analysis, and histochemical tests were performed to locate and identify classes of chemical compounds. The distinctive features identified were low concentration of crystal sand in the root and stem, presence of terpene resin in the root, and absence of hypodermis in the leaf, in *S. agrarium*; bright spots (group of sclereids) in the root, isobilateral mesophyll, thickened cell walls with hemicelluloses and strong aroma in the fruit, in *S. lycocarpum*; high concentration of crystal sand in the root and stem, oval-shaped limb, presence of isolated crystals in the exocarp, in *S. palinacanthum*; strong sclerification and rays with great height in the root and stem, in *S. paniculatum*; and accumulation of soluble protein in the root and stem, presence of conspicuous membranaceous stipules, absence of spiniform trichomes, in *S. stipulaceum*. This work identifies distinctive structural features, its ecological importance, and determines the distribution of secondary compounds associated with the medicinal properties reported for these species and contributes to the conservation of the natural environments where they occur.

Introduction

The botanical and chemical characterization of medicinal species is important for the validation of its traditional use and for studies to obtaining new products and innovation (Araújo et al., 2010; Nurit-Silva et al., 2011; WHO, 2013). The structural analysis of plants identifies distinctive features useful for the determination of the authenticity of medicinal plant species and the identification of the plant organs where the highest concentrations of active substances are present, especially when the plants are fragmented for use in herbal drugs (Argyropoulou et al., 2010; Ferreira et al., 2011; Coelho et al., 2012). These features have an ecological function, related to the environment where the plant occurs. The understanding of this function may help optimize their cultivation and collection (Adams et al., 2013; Moreira et al., 2013; Sampaio et al., 2014).

Chemical studies performed using histochemical techniques allow a quick and inexpensive preliminary evaluation of the medicinal potential of taxonomically close species in the search for new pharmaceuticals (Coelho et al., 2012; Demarco et al., 2013; Araújo et al., 2014; Mercadante-Simões et al., 2014). This technique can minimize costs in the search for new pharmaceuticals and increase the safety of traditional medicines (Adams et al., 2013; Santos et al., 2013), however histochemical studies are rare in *Solanum* (Araújo et al., 2010; Picoli et al., 2013).

Solanaceae is widely distributed with 269 species of the genus *Solanum* L. described in Brazil (Stehmann et al., 2014). Some of the species occurring in the Cerrado biome are traditionally used for the control of diabetes, and have been recognized for their medicinal properties: *Solanum agrarium* Sendtn. has anti-inflammatory effects (Agra et al., 2007; Castro et al., 2011), *S. lycocarpum* A. St.-Hil is hypoglycemic (Farina et al., 2010), *S. palinacanthum* Dunal is used as antimicrobial and hypoglycemic (Pereira et al., 2008), *S. paniculatum* L. has antioxidant and anticarcinogenic action (Ribeiro et al., 2007; Endringer et al., 2010), and *S. stipulaceum* Roem. & Schult. is used as a blood pressure regulator (Ribeiro et al., 2002).

* Corresponding author.
E-mail: maria.simoes@unimontes.br (M.O. Mercadante-Simões).

http://dx.doi.org/10.1016/j.bjp.2015.11.002
0102-695X/

Most pharmacognostic analyses in *Solanum* species were performed on leaves of only one or two species (Araújo et al., 2010; Nurit-Silva et al., 2011), and anatomical studies on a larger number of species are on taxonomy (Sampaio et al., 2014; Nurit-Silva et al., 2012). Therefore the goal of the present study was to identify distinctive structural features on the root and stem barks, leaves and pericarps of *S. agrarium*, *S. lycocarpum*, *S. palinacanthum*, *S. paniculatum*, and *S. stipulaceum*, its ecological importance, determine the distribution of secondary compounds associated with the medicinal properties reported for these species and contribute to the conservation of the natural environments where they occur.

Materials and methods

Plant material

Fragments of root and stem (apices and bark, considering bark the tissues external to the vascular cambium, *sensu* Fahn, 1990), leaf, pericarp, and root and stem apexes were collected from three

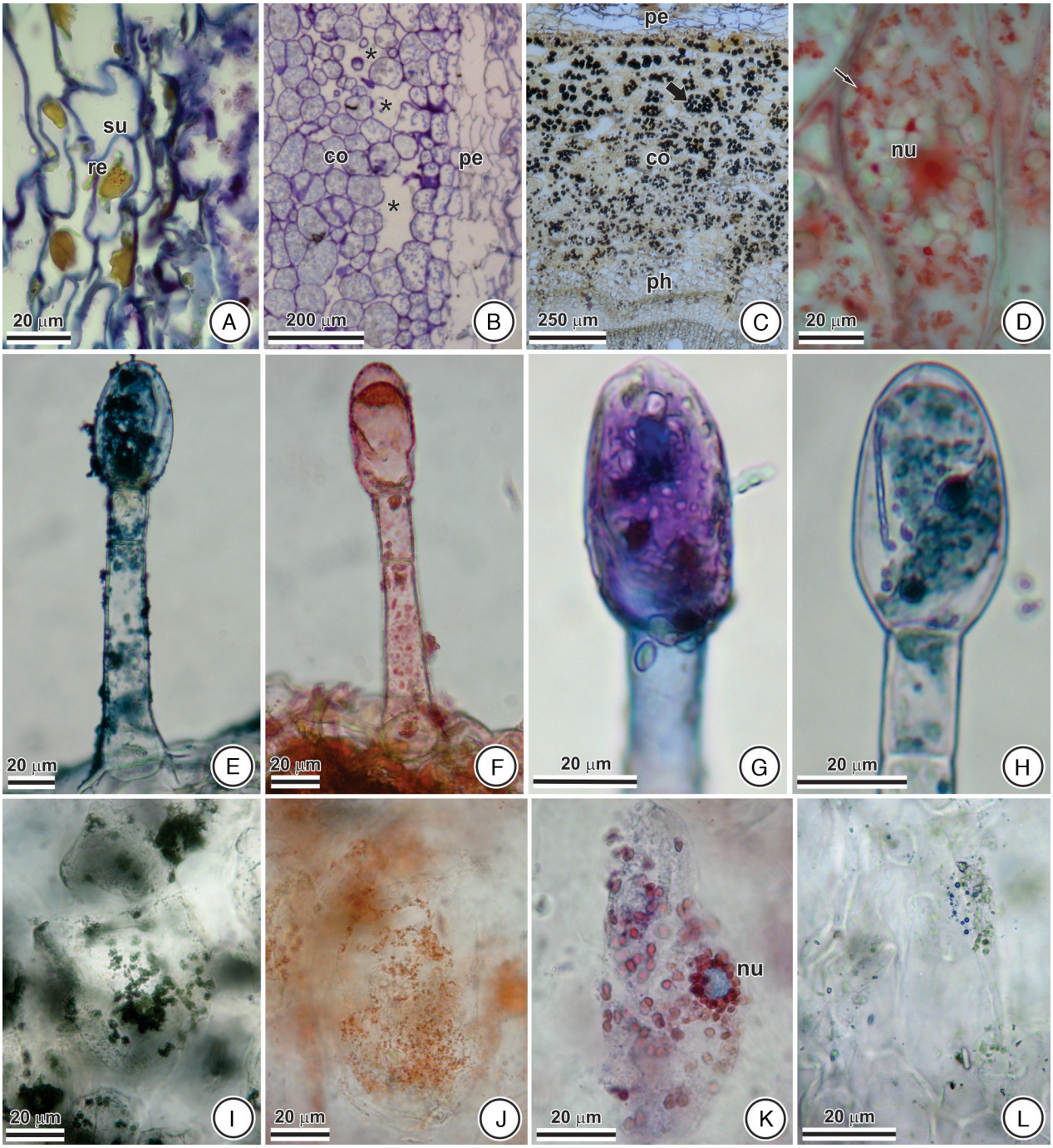

Fig. 1. Structural and histochemical features of *Solanum agrarium* Sendt. (A, C–L) Cross sections and (B) radial longitudinal section. (A–D) Root. (A) Suber with resin accumulation. (B) Voluminous intercellular spaces (asterisk). (C) Cortex with starch accumulation stained black with Lugol (arrow). (D) Cortex with protein reserve (arrow) stained red with XP. (E–H) Leaf with lipophilic compounds in the glandular trichome, with a long stalk. (E) Black with Sudan B black. (F) Red with Sudan IV. (G) Blue and lilac with Nile blue. (H) Blue with NADI. (I–L) Mesocarp with lipophilic compounds. (I) Black with Sudan B black. (J) Orange with Sudan IV. (K) Pink with Nile blue. (L) Blue with NADI. (co) cortex, (nu) nucleus, (pe) periderm, (ph) phloem, (re) resin, (su) suber.

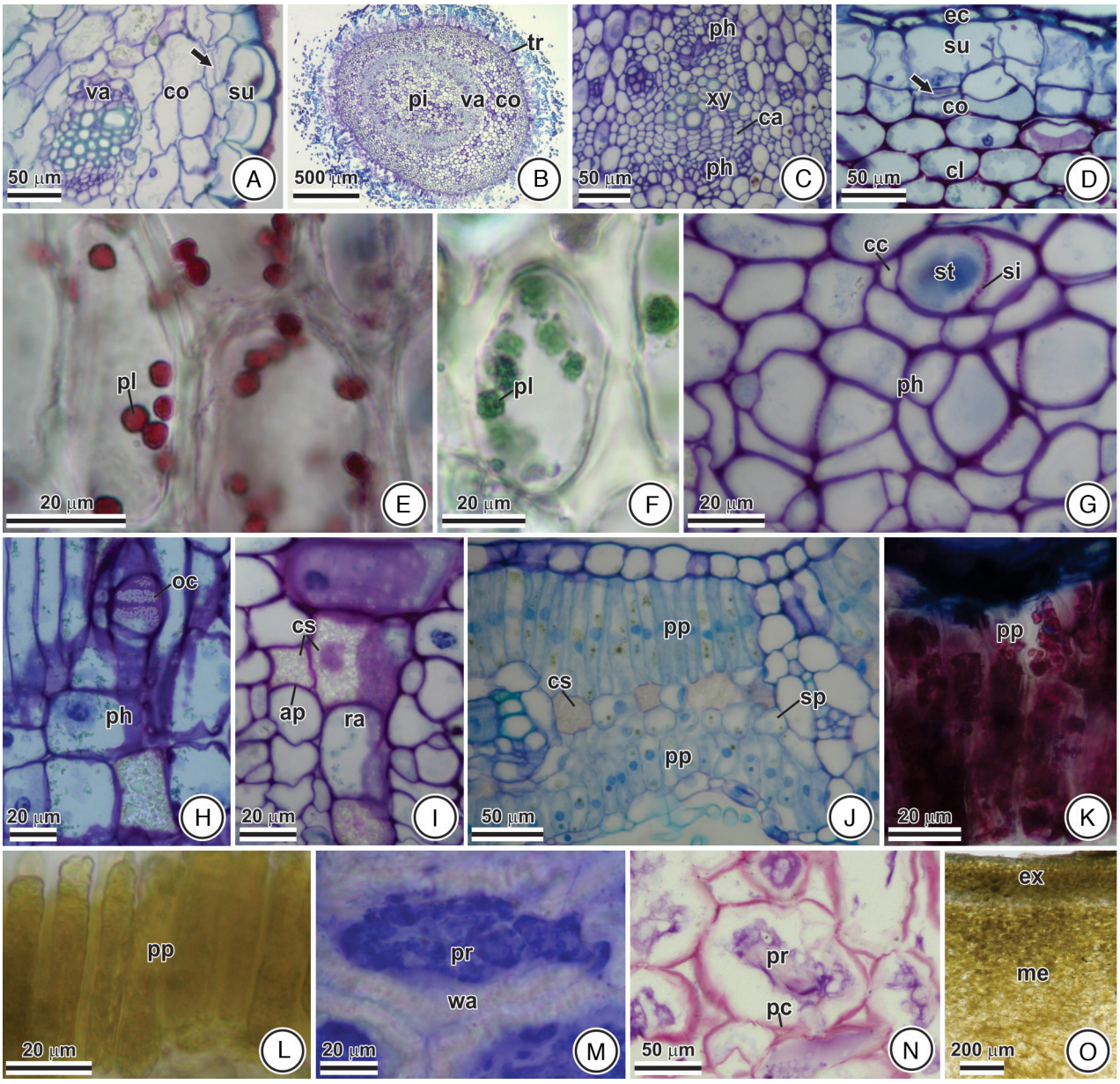

Fig. 2. Structural and histochemical features of *Solanum lycocarpum* A. St.-Hil. (A–G, I–L, N, O) Cross sections. (H, M) Radial longitudinal section. (A) Root primary structure showing settlement of phellogen at the cortex (arrow). (B–I) Stem. (B) Primary structure with high density of tector trichomes. (C) Bicollateral bundle. (D) Settlement of phellogen at the cortex (arrow). (E and F) Cortical cells with plastids presenting terpenoids. (E) Pink with Nile blue. (F) Blue with NADI. (G) Sieve tube elements of large diameter. (H) Oblique compound sieve plates. (I) Accumulation of crystal sand in the rays and axial parenchyma. (J–L) leaf. (J) Isobilateral mesophyll presenting crystal sand. (K and L) Palisade parenchyma. (K) Lipids stained pink with Nile blue. (L) Alkaloids stained yellow with Ellram reagent. (M–O) Pericarp. (M) Mesocarp cells presenting cellulose walls with pronounced thickness. (N) Low pectin concentration in mesocarp cell walls. (O) Exocarp and mesocarp with alkaloids stained brown with Dragendorff. (ap) axial parenchyma, (ca) cambium, (cc) companion cell, (cl) collenchyma, (co) cortex, (cs) crystal sand, (ec) epidermis cell, (ex) exocarp, (me) mesocarp, (oc) oblique compound plate, (pc) pectin, (ph) phloem, (pi) pith, (pl) plastids, (pp) palisade parenchyma, (pr) protoplast, (ra) ray, (si) sieve plate, (sp) spongy parenchyma, s(t) sieve tube element, (su) suber, (tr) tector trichome, (va) vascular bundle, (xy) xylem, (wa) wall.

individuals of *Solanum agrarium* Sendtn., *S. lycocarpum* A. St.-Hil., *S. palinacanthum* Dunal, *S. paniculatum* L., and *S. stipulaceum* Roem. & Schult., occurring in the Brazilian Cerrado, in the municipality of Montes Claros (16°50′06.1″ S, 43°55′24.8″ W; 16°30′53.2″ S, 44°04′28.0″ W). Vouchers were obtained from fertile material and deposited at the BHCB Herbarium of the Departamento de Botânica, do Instituto de Ciências Biológicas, da Universidade Federal de Minas Gerais, Brazil (116081, 168587-168590; LL Giacomin).

Structural characterization

Morphological analysis was performed on all fresh plant material using a binocular stereo-microscope, model 0766ZL (Motic, Richmond, Canada) according to nomenclature proposed by Junikka (1994). For structural analysis, the plant material was evaluated fresh or fixed in Karnovsky solution (Karnovsky, 1965) for 12 h, dehydrated in a graded ethanol series (Jensen, 1962), and cold-embedded (Paiva et al., 2011) in hydroxyethyl-methacrylate resin (Leica Microsystem Inc., Heidenbeg, Germany). Cross sections and parademic sections were obtained using a LPC table microtome (Rolemberg and Bhering, Belo Horizonte, Brazil). Cross sections and longitudinal sections, 5 μm thick, were obtained using a rotary microtome (Atago, Tokyo, Japan). The sections were stained with toluidine blue pH 4.7 (O'Brien et al., 1964, modified), and mounted in acrylic resin (Itacril, Itaquaquecetuba, Brazil).

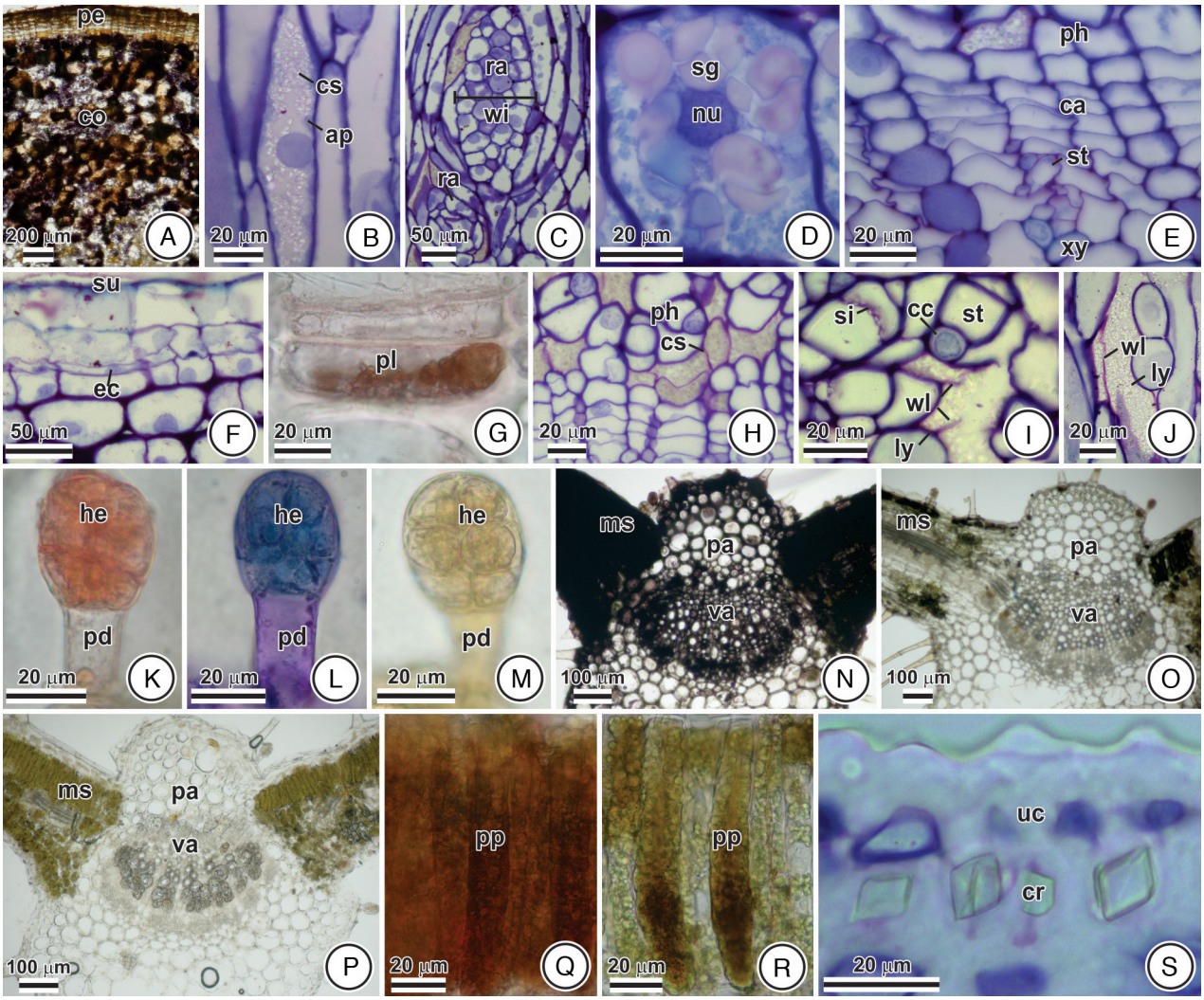

Fig. 3. Structural and histochemical features of *Solanum palinacanthum* Dunal. (A, D–I, K–S) Cross sections. (B–C, J) (tangential longitudinal sections. (A–E) Root bark. (A) Cortex with alkaloids stained brown with Dragendorff. (B) Axial parenchyma with crystal idioblast. (C) Wide rays. (D) Starch reserve in radial cell. (E) Formation of conducing elements at the cambium. (F–J) Stem bark. (F) Establishment of phellogen at the epidermis. (G) Phelloderm presenting flavonoids stained red with DMACA. (H) Crystal sand at the phloem. (I and J) Formation of lysigenous duct containing crystal sand. (K–R) Leaf. (K–M) Short glandular trichome. (K) Mucilage stained red with XP. (L) Lipids stained blue with Nile blue. (M) Phenol stained brown with iron chloride. (N–P) Median vein. (N) Mucilage stained black with tannic acid. (O) Phenols stained brown with iron chloride. (P) Alkaloids stained yellow with Ellram. (Q-R) Palisade parenchyma. (Q) Flavonoids stained red with DMACA. (R) Alkaloids stained yellow-brown with Dittmar. (S) Exocarp with undulated cuticle and single crystals. (ap) axial parenchyma, (ca) cambium, (cc) companion cell, (co) cortex, (cr) crystals, (cs) crystal sand, (ec) epidermis cell, (he) head, l(y) lysigenous duct, (ms) mesophyll, (nu) nucleus, p(a) parenchyma, (pe) periderm, (ph) phloem, (pl) phelloderm, (pp) palisade parenchyma, (ra) ray, (si) sieve plate, (sg) starch grains, (st) sieve tube element, (su) suber, (pd) peduncle, (uc) undulated cuticle, (va) vascular bundle, (wi) width, (wl) cell wall lysis, (xy) xylem.

Histochemical tests

Histochemical tests were performed on sections obtained from fresh material as described above using the following reagents: Lugol (Johansen, 1940) for detection of starch, tannic acid (Pizzolato and Lillie, 1973) and ruthenium red (Johansen, 1940) for acid polysaccharides, xylidine Ponceau (XP) (Vidal, 1970) and Coomassie blue (Fisher, 1968) for protein, Sudan red IV and Sudan black B (Pearse, 1980) for total lipophilic compounds, Nile blue (Cain, 1947) for acid and neutral lipids, α-naphthol and dimethylparaphenylenediamine hydrochloride (NADI) (David and Carde, 1964) for essential oils and oleoresins, Ellram, Dittmar (Furr and Malhberg, 1981), and Dragendorff reagents (Svendsen and Verpoorte, 1983) for alkaloids, potassium dichromate (Gabe, 1968) and iron chloride (Johansen, 1940) for phenols; vanillin chloride (Mace and Howell, 1974) for tannins; and *p*-dimethylaminocinnamaldehyde (DMACA) (Feucht et al., 1986) for flavonoids. Control tests were performed simultaneously according to the recommendations of the respective authors.

Photographic documentation was performed using an AxioCam MRc camera coupled to an AxioVision LE photomicroscope (Zeiss, Oberkochen, Germany) and an A 620 digital camera (Canon, Tokyo, Japan) coupled to a Eclipse E-200 light microscope (Nikon, Tokyo, Japan).

Results

Structural and histochemical characters reported for the four organs of the five species of *Solanum* are presented by species, in Figs. 1–5, and by organs in Tables 1–8. The data presented by species can contribute to the elaboration of monographs, and presented by the organs are to contribute to the quality control of the drug obtained from the species.

S. agrarium presented root bark with a corrugated internal texture, resin accumulation at the suber, voluminous intercellular spaces, low lignification, and considerable starch and protein reserves (Fig. 1A–D and Tables 1 and 2). The stem bark had a strong

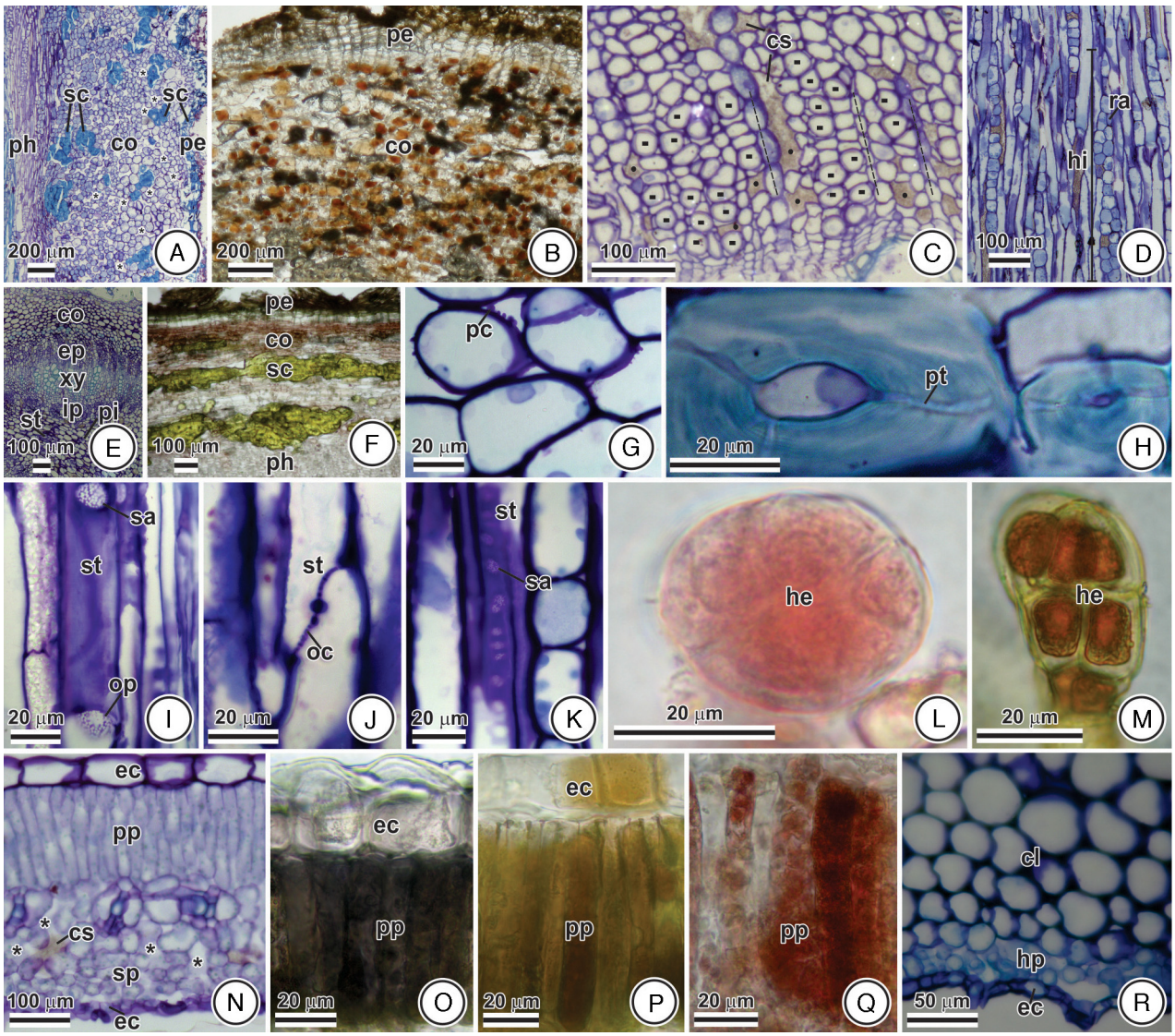

Fig. 4. Structural and histochemical features of *Solanum paniculatum* L. (A, G–I) Longitudinal radial sections. (B, C, E, F, L–R) Cross sections. (D, J–K) Tangential longitudinal sections. (A–D) Root bark. (A) Sclerified cortex with voluminous intercellular spaces (asterisk). (B) Cortex with phenols stained brown with dichromate. (C) Phloem with higher proportion of conducing elements (rectangle) than the axial parenchyma (circle) and close rays (dotted line). (D) High radial height. (E–H) stem bark. (E) Sieve tube elements at the pith. (F) Cortex with flavonoids stained red with DMACA. (G) Pectin projections in cortical cells. (H) Sclereids with observable pit. (I–K) sieve tube elements. (I) Oblique plates. (J) Compound plates. (K) Small-diameter sieve areas. (L–R) leaf. (L–M) Glandular trichome. (L) Alkaloids stained brown with Dittmar. (M) Mucilage stained red with XP. (N) Dorsiventral mesophyll. (O–Q) palisade parenchyma, o mucilage stained black with tannic acid. (P) Phenols stained brown with dichromate. (Q) Flavonoids stained red with DMACA. (R) Lignified hypodermis at the abaxial surface of the median vein. (cl) collenchyma, (co) cortex, (cs) crystal sand, (ec) epidermis cell, (ep) external phloem, (ip) internal phloem, (he) head, (hi) height, (hy) hypodermis, (oc) oblique compound plate, (op) oblique plate, (pc) pectin, (pe) periderm, (ph) phloem, (pi) medulla, (pp) palisade parenchyma, (pt) pit, (ra) ray, (sa) sieve areas, (sc) sclerification, (sp) spongy parenchyma, (st) sieve tube element, (xy) xylem.

bitter taste and low sclerification; the cortex had voluminous intercellular spaces, high starch accumulation, and a small quantity of crystal sand; the volume occupied by the axial parenchyma was significantly larger than that of the sieve tube elements at the phloem (Tables 3 and 4). Leaves presented a median vein composed of polyhedric epidermis cells, no hypodermis, and accumulation of terpenoids in the secretory trichomes; the lower-caliber vascular bundles at the petiole were collateral and not surrounded by pericyclic fibers (Fig. 1E–H and Table 5). The exocarp was purple, and alkaloids and terpenoids accumulated at the mesocarp (Fig. 1I–L and Tables 7 and 8).

In *S. lycocarpum*, the establishment of phellogen in the root at the peripheral cortical cells, and the secondary phloem presented a compact arrangement of axial parenchyma, homogeneous ray height, and sieve tube elements with diminute caliber and pores (Fig. 2A and Tables 1 and 2). The stem in primary structure was pilous; the stem bark presented lenticels and cuboid-shaped suber cells; the cortex accumulated terpenoids; and the phloem had thin-walled sieve tube elements (Fig. 2B–I and Tables 3 and 4). The mesophyll was isobilateral. The median vein region presented epidermal cells with straight anticlinal walls, accumulation of crystal sand, and high sclerification index (Fig. 2J–L and Table 5). The fruit had a strong aroma, the exocarp exhibited thick collenchyma, and the cells of the mesocarp had thick walls with low concentration of pectin but high concentration of mucilage, protein, and starch, and an alkaloid-rich protoplast (Fig. 1M–O and Tables 7 and 8).

S. palinacanthum presented significant accumulation of alkaloids and crystal sand at the root bark and phloem rays with large variation in width (Fig. 3A–E and Tables 1 and 2). The stem bark had phloem with short rays, and significant accumulation of mucilage, tannins, flavonoids, alkaloids, and crystal sand (Fig. 3F–J and Tables 3 and 4). The leaf limb was oval-shaped with a cordate basis.

Table 1
Structural features of root of *Solanum agrarium* Sendtn., *Solanum lycocarpum* A. St.-Hil., *Solanum palinacanthum* Dunal, *Solanum paniculatum* L., and *Solanum stipulaceum* Roem. & Schult.

Features	*Solanum* species				
	ag	ly	pl	pn	st
Morphology					
Bitter taste	1	1	2	1	2
External surface					
Texture	wr	ro	wr	ro	ro
Color	br	br	br	br	br
Internal surface					
Corrugated texture	2	1	1	1	1
Periderm cross section					
Color	br	br	br	br	br
Thickness	1	2	1	2	2
Cortex/phloem					
Color	ye	ye	ye	ye	ye
Bright spots	1	2	1	1	1
Anatomy					
Primary structure					
Epidermis					
Cell shape	tb	tb	tb	tb	tb
Phellogen establishment	el	el	el	el	el
Cortex					
Intercellular space	2	1	1	1	1
Cell shape	tb	tb	tb	tb	tb
Crystal sand	0	1	2	0	0
Endophytic fungi	2	1	2	1	2
Vascular system	di	di	di	di	di
Secondary structure					
Periderm					
Suber					
Cell shape	tb	tb	tb	cu	tb
Cell wall thickening	1	1	1	1	1
Sclerification	0	0	0	2	0
Resin	2	1	1	0	0
Phelloderm					
Thickness	1	1	1	1	1
Crystal sand	0	0	1	1	1
Sclereids	0	0	0	1	1
Cortex					
Thickness	2	2	2	2	1
Intercellular spaces	2	1	1	1	1
Crystal sand	1	1	2	1	1
Sclereids	0	1	1	2	1
Phloem					
Primary phloem fibers	1	0	1	0	1
Pseudocortex	1	0	1	1	2
Sclerification	0	2	1	1	1
Sieve tube elements					
Quantity	1	1	1	2	1
Wall thickening	2	1	2	2	2
Caliber	2	1	2	2	2
Length	1	1	1	1	1
Distribution	rb	rb	rb	rb	rb
Plates	oc	oc	oc	oc	oc
Sieve diameter	2	1	2	2	2
Sieve areas					
Quantity	1	1	1	1	2
Diameter	2	1	2	2	2
Axial parenchyma					
Volume	2	2	2	1	2
Caliber	2	2	2	1	2
Crystal sand	1	1	2	2	2
Ray					
Width	1–2	1–2	1–8	1–3	1–3
Height	6–20	12–14	1–11	10–25	1–12
Crystal sand	1	1	1	2	1

(ag) *S. agrarium*, (br) brown, (cu) cuboids, (di) diarch, (el) external layers (epidermis/cortex), (ly) *S. lycocarpum*, (oc) oblique compound, (pl) *S. palinacanthum*, (rb) radial bands, (ro) rough, (pn) *S. paniculatum*, (st) *S. stipulaceum*, (tb) tabular, (wr) wrinkled, (ye) yellow, (0) absent, (1) moderate, (2) pronounced.

The mesophyll accumulated tannins, had acid polysaccharide-rich cell walls, and showed annular collenchyma at the median vein cortex (Fig. 3K–R and Tables 5 and 6). Its exocarp was yellow and had single crystals at the epidermis; its mesocarp had a light white color, voluminous intercellular spaces, and alkaloid-rich cells (Fig. 1S and Tables 7 and 8).

S. paniculatum presented strong aggregation of sclereids, observable under stereomicroscope as bright spots, at the suber and

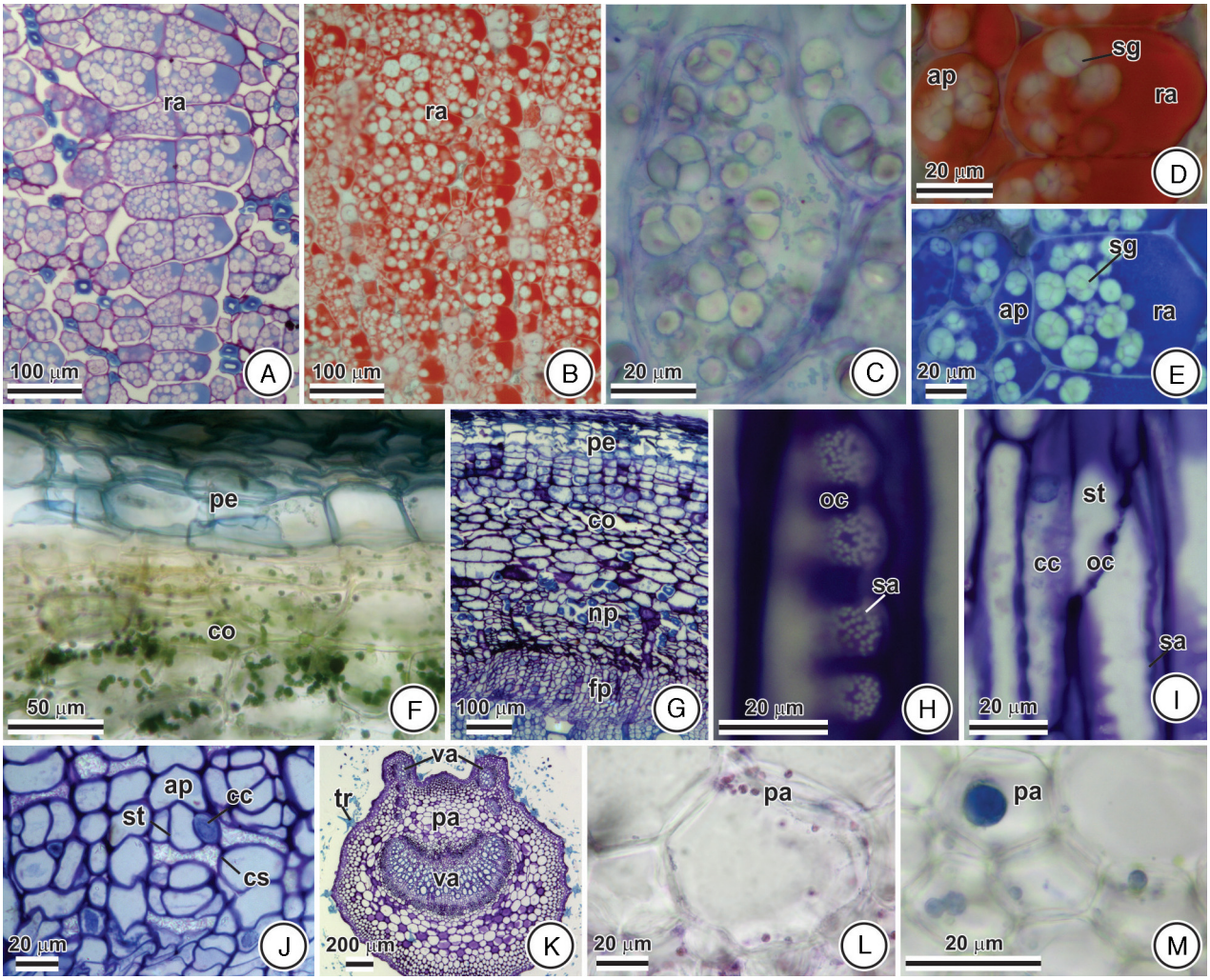

Fig. 5. Structural and histochemical features of *Solanum stipulaceum* Roem. & Schult. (A–G, J–M) Cross sections. (H and I) Tangential longitudinal sections. (A–E) root bark. (A) Tangential expansion (dotted line) of ray forming the pseudocortex. (B–E) Protein accumulation at the phloem parenchyma. (B, D) Stained red with XP. (C, E) Stained blue with Coomassie blue. (C) Control test. (F–J) Stem bark. (F) Lipids at the external cortex stained black with Sudan black B. (G) Evident annual rings. (H) Oblique compound plates with several sieve areas. (I) Lateral sieve areas with large diameter. (J) Axial parenchyma presenting cells with large caliber. (K–M) Leaf. (K) Petiole with tector trichomes. (L–M) terpenoids at the vein. (L) Pink and blue with Nile blue. (M) Blue with NADI. (ap) axial parenchyma, (cc) companion cell, (co) cortex, (cs) crystal sand, (fp) functional phloem, (np) non-conducting phloem, (oc) oblique compound plates, (pa) parenchyma, (pe) periderm, (ra) ray, (sa) sieve areas, (sg) starch grains, (st) sieve tube element, (tr) tector trichome, (va) vascular bundle.

Table 2
Histochemical features of root of *Solanum agrarium* Sendtn., *Solanum lycocarpum* A. St.-Hil., *Solanum palinacanthum* Dunal, *Solanum paniculatum* L., and *Solanum stipulaceum* Roem. & Schult.

	Test	Suber					Feloderm/cortex					Phloem				
		ag	ly	pl	pn	st	ag	ly	pl	pn	st	ag	ly	pl	pn	st
Primary metabolites																
Starch	Lugol	0	0	0	0	0	2	1	1	1	1	2	1	1	1	1
Acidic polysaccharides	Tannic acid	0	0	0	0	0	1	1	1	1	1	1	1	1	1	1
	Rhutenium red	1	1	1	1	1	1	1	1	1	1	1	1	1	1	1
Proteins	XP	0	0	0	0	0	1	1	1	1	2	1	1	1	1	2
	Coomassie blue	0	0	0	0	0	1	1	1	1	2	1	1	1	1	2
General lipid	Sudan VI	1	1	1	1	1	1	1	0	1	0	1	1	1	1	0
	Sudan black	1	1	1	1	1	1	1	0	1	0	1	1	1	1	0
Neutral lipids	Nile blue	1	1	1	1	1	1	1	0	0	0	1	0	1	0	0
Acids lipids		1	1	1	1	1	1	1	0	1	0	1	1	1	1	0
Secondary metabolites																
Terpenoids	NADI	2	0	0	0	0	0	0	0	0	0	0	1	0	1	0
Alkaloids	Ellram	0	0	0	0	0	0	0	1	0	1	0	0	0	0	0
	Dittmar	0	0	0	0	0	1	1	1	1	2	1	1	1	0	1
Phenolic compounds	Dicromato	0	0	0	0	0	1	1	1	2	1	1	0	1	1	0
Tannins	Vanillin	0	0	0	0	0	1	1	1	1	1	0	1	0	0	1
Flavonoids	DMACA	0	0	0	0	0	1	1	1	1	1	0	1	0	0	0

(ag) *S. agrarium*, (ly) *S. lycocarpum*, (pl) *S. palinacanthum*, (pn) *S. paniculatum*, (st) *S. stipulaceum*, (0) absent, (1) moderate, (2) pronounced.

Table 3
Structural features of stem of *Solanum agrarium* Sendtn., *Solanum lycocarpum* A. St.-Hil., *Solanum palinacanthum* Dunal, *Solanum paniculatum* L., and *Solanum stipulaceum* Roem. & Schult.

Features	*Solanum* species				
	ag	ly	pl	pn	st
Morphology					
Bitter taste	2	1	1	1	1
External surface					
Color	db	br	gr	gr	gr
Trichomes	2	0	2	2	2
Textura	sm	ro	wr	wr	sm
Lenticels	1	0	2	2	2
Thorns	1	1	1	1	0
Internal surface					
Corrugated texture	1	1	1	1	2
Periderm cross section					
Color	br	br	br	br	br
Thickness	1	1	1	1	1
Anatomy					
Primary structure					
Epidermis					
Cell shape	cu	cu	cu	cu	cu
Tector trichomes					
Quantity	1	2	0	0	1
Ramification	0	1	0	0	1
Glandular trichomes					
Quantity	0	0	1	0	0
Head	0	0	mc	0	0
Peduncle	0	0	sh	0	0
Cortex/phloem					
Anelar collenchyma	1	1	1	1	1
Cortical parenchyma					
Thickness	2	2	2	1	2
Intercellular spaces	0	0	0	2	0
Cell shape	ov	gl	gl	ov	gl
Crystal sand	0	1	1	2	2
Vascular system	bi	bi	bi	bi	bi
Pericyclic fibers	0	0	0	0	2
Crystal sand	0	0	0	2	2
Vascular bundle	bi	bi	bi	bi	bi
Medullary parenchyma					
Sclereids	0	0	0	0	2
Crystal sand	0	1	1	0	2
Secondary structure					
Periderm					
Suber					
Cell shape	ta	cu	ta	ta	ta
Cell wall thickening	1	1	1	1	1
Resin	1	1	0	0	0
Phellogen installation	ep	co	ep	ep	co
Phelloderm					
Thickness	1	1	1	1	1
Crystal sand	0	0	0	0	1
Sclereids	0	0	0	0	1
Cortex					
Thickness	1	2	1	1	1
Colenchyma	1	1	1	0	1
Parenchyma					
Intercellular spaces	2	1	1	1	1
Crystal sand	1	1	2	1	1
Sclereids	0	1	1	2	1
Phloem					
Sieve tube elements					
Quantity	1	2	2	2	2
Wall thickening	2	1	2	2	2
Caliber	1	2	1	2	1
Length	1	1	1	1	1
Distribution	rb	rb	rb	rb	rb
Sieve plate	oc	oc	oc	oc	oc
Sieve areas					
Quantity	1	1	1	1	2
Diameter	1	1	1	1	1
Sieve diameter	1	1	1	1	1

Table 3 (*Continued*)

Features	*Solanum* species				
	ag	ly	pl	pn	st
Axial parenchyma					
Volume	2	1	1	1	1
Caliber	2	2	2	2	2
Crystal sand	1	1	2	1	2
Ray					
Width	1	1–2	1–2	1–2	1–2
Height	10–15	14–20	3–7	5–30	6–16
Crystal sand	1	1	0	1	0
Sclerenchyma	0	2	1	2	2

(ag) *S. agrarium*, (bi) bicolateral, (br) brown, (bs) black spots, (co) cortex, (cu) cuboid, (db) dark brown, (ep) epidermis, (gl) globoid, (gr) green, (ly) *S. lycocarpum*, (mc) multicellular, (oc) oblique compound, (ov) ovoid, (pl) *S. palinacanthum*, (pn) *S. paniculatum*, (rb) radial bands, (ro) rough (sh) short, (sm) smooth, (ta) tabular, (st) *S. stipulaceum*, (wr) wrinkled, (0) absent, (1) moderate, (2) pronounced.

cortex of the root bark; the phloem presented numerous sieve tube elements and rays with large height (Fig. 4A–D and Tables 1 and 2). The stem bark presented alkaloid accumulation at the cortex and voluminous sclereids; the bicollateral vascular bundles presented internal phloem penetrating deeply into the medulla, and rays of large height at the phloem (Fig. 4E–K and Tables 3 and 4). Heterophylly was pronounced; the mesophyll had voluminous intercellular spaces, and temporary cellular accumulation of starch and flavonoids (Fig. 4L–R and Tables 5 and 6). Accumulation of soluble sugars was observed in the fruit, which conferred a sweet taste to the pericarp (Tables 7 and 8).

S. stipulaceum is the most distantly species to the other studied species. The root bark developed a voluminous pseudocortex with evenly spaced rays, it was rich in soluble protein reserves, and was oriented adjacent to the phloem axial elements. The axial parenchyma was voluminous (Fig. 5A–E and Tables 1 and 2). The stem bark had no spiniform trichomes, and the internal surface was corrugated. The phloem presented accumulation of terpenoids, well-defined annual rings, and sieve tube elements with plates presenting numerous sieve areas (Fig. 5F–J and Tables 3 and 4). The leaves presented large membranaceous stipules that were distinctive morphological features easily observable, and accumulation of terpenoids (Fig. 5K–M and Tables 5 and 6). The fruit was notable for the accumulation of tannins (Tables 7 and 8).

The data presented in Figs. 1–5 and Tables 1–8 show structural characters useful for identification and adaptation of the studied species to the environment where they occur, and chemical compounds related to their therapeutic use: (a) in *S. agrarium*, low concentration of crystal sand in the root and stem, the presence of terpene resin in the root, and absence of hypodermis in the leaf; (b) in *S. lycocarpum*, bright spots (group of sclereids) in the root, isobilateral mesophyll, thickened cell walls with hemicelluloses and strong aroma in the fruit; (c) in *S. palinacanthum*, high concentration of crystal sand in the root and stem, oval-shaped limb, and presence of isolated crystals in the exocarp; (d) in *S. paniculatum*, strong sclerification in the root and stem, and rays with great height; and (e) in *S. stipulaceum*, accumulation of soluble protein in the root and stem, presence of conspicuous membranaceous stipules, and absence of spiniform trichomes.

Discussion

Structural data on medicinal plant are secure characters for species identification and quality control of plant drug and reveal their relationship with the environment. Roots, stems, leaves and fruits, dehydrated and fragmented are widely used as herbal drugs. They may be substituted for each other resulting in fraud in the preparation of herbal medicines (Adams et al., 2013).

The phellogen establishment at the root and stem constitute an important distinctive feature for these organs. At the roots, the formation of periderm always starts at the more peripheral cortical layers (Metcalfe and Chalk, 1957). The vascular bundles in all studied species in this work were bicollateral, that is a characteristic of Solanaceae and the occurrence of intramedullary phloem bundles, situated deeply in the pith, in *S. paniculatum* has been reported for species of other genera of Solanaceae (Metcalfe and

Table 4
Histochemical features of stem *Solanum agrarium* Sendtn., *Solanum lycocarpum* A. St.-Hil., *Solanum palinacanthum* Dunal, *Solanum paniculatum* L., and *Solanum stipulaceum* Roem. & Schult.

	Test	Suber					Feloderm/cortex					Phloem				
		ag	ly	pl	pn	st	ag	ly	pl	pn	st	ag	ly	pl	pn	st
Primary metabolites																
Starch	Lugol	0	0	0	0	0	2	1	1	1	1	2	1	1	1	1
Acidic polysaccharides	Tannic acid	0	0	0	0	0	1	1	1	1	1	1	1	1	1	1
	Ruthenium red	1	1	1	1	1	1	1	1	1	1	1	1	1	1	1
Proteins	XP	0	0	0	0	0	1	1	1	1	1	1	1	1	1	1
	Coomassie blue	0	0	0	0	0	1	1	1	1	1	1	1	1	1	1
General lipid	Sudan VI	1	1	1	1	1	1	1	1	1	1	1	1	1	1	1
	Sudan black	1	1	1	1	1	1	1	1	1	1	1	1	1	1	1
Neutral lipids	Nile blue	1	1	1	1	1	1	1	1	1	1	1	1	1	1	1
Acids lipids		1	1	1	1	0	0	0	0	1	0	0	0	0	1	0
Secondary metabolites																
Terpenoids	NADI	1	1	1	1	1	1	0	0	1	1	1	0	0	1	1
Alkaloids	Ellram	0	0	0	0	0	1	0	0	1	0	1	0	1	0	0
	Dittmar	0	0	0	0	0	1	0	0	1	0	1	0	1	0	0
Phenolic compounds	Dichromate	0	0	0	0	0	1	1	1	1	1	1	1	0	1	1
Tannins	Vanillin	0	0	0	0	0	0	1	1	0	0	0	0	0	0	0
Flavonoids	DMACA	0	0	0	0	0	1	1	1	1	1	1	1	1	1	1

(ag) *S. agrarium*, (ly) *S. lycocarpum*, (pl) *S. palinacanthum*, (pn) *S. paniculatum*, (st) *S. stipulaceum*, (0) absent, (1) moderate, (2) pronounced.

Table 5
Leaf structural features of *Solanum agrarium* Sendtn., *Solanum lycocarpum* A. St.-Hil., *Solanum palinacanthum* Dunal, *Solanum paniculatum* L., and *Solanum stipulaceum* Roem. & Schult.

Features	*Solanum* species				
	ag	ly	pl	pn	st
Morphology					
Phyllotaxis	at	at	at	at	at
Stipule	0	0	0	0	1
Heterophylly	1	1	1	2	1
Petiole	1	1	1	1	1
Limb	si	si	si	si	si
Shape	el	el	ov	el	el
Margin	pi	pi	pi	wh	wh
Apex	ac	ac	ac	am	am
Base	ol	ol	cd	ol	cn
Consistency	hb	hb	hb	hb	hb
Surface	sm	sm	sm	sm	sm
Pilosity	1	2	1	2	2
Nervation	pn	pn	pn	pn	pn
Anatomy					
Intervein region					
Trichomes					
Spiniform	2	1	2	1	0
Tectors					
Quantity	1	2	1	2	2
Ramification	0	1	0	1	1
Glandular					
Short erect					
Quantity	0	0	2	2	2
Head	0	0	mu	mu	mu
Long erect					
Quantity	1	0	1	0	0
Head	un	0	un	0	0
Bent					
Quantity	2	0	2	1	2
Head	mu	0	un	mu	mu
Epidermis					
Cell shape	t	t	t	t	t
Undulation of anticlinal walls	1	1	0	2	0
Mesophyll	dv	is	dv	dv	dv
Crystal sand	0	1	1	1	1
Palisade parenchyma					
Number of layers	1	1	1	1	1
Cell length	he	he	ho	ho	ho
Spongy parenchyma					
Intercellular spaces	1	1	1	2	1
Vascular bundle	bi	bi	bi	bi	bi
Median vein					
Epidermis					
Cell shape	po	cb	cb	cb	cb
Undulation of anticlinal walls	2	0	1	2	1
Hypodermis	0	1	1	1	1
Collenchyma	1	2	2	2	2
Type	an	an	al	an	an
Crystal sand	0	1	1	1	0
Sclereids	0	1	0	0	0
Parenchyma					
Crystal sand	0	2	1	1	1
Sclereids	0	1	0	0	0
Vascular bundle	bi	bi	bi	bi	bi
Pericyclic fibers	2	2	1	0	0
Crystal sand	0	1	1	1	1
Petiole					
Epidermis					
Cell shape	cb	cb	cb	cb	cb
Undulation of anticlinal walls	1	0	1	0	0
Collenchyma	1	2	2	2	2
Wall thickening	an	an	al	an	an
Parenchyma					
Crystal sand	1	2	2	2	1
Intercellular spaces	1	2	2	1	1
Sclereids	0	1	0	0	0
Vascular system shape	hm	hm	hm	hm	hm
Pericyclic fibers	0	2	0	0	0
Crystal sand	0	1	1	1	1
Lower caliber bundles	co	bi	bi	bi	bi

(ac) acute, (ag) *S. agrarium*, (al) annulate, (am) acuminate, (an) angular, (at) alternate, (bi) bicollateral, (cb) cuboid, (cd) cordate, (cn) cuneiform, (co) collateral, (dv) dorsiventral, (el) elliptical, (hb) herbaceous, (he) heterogeneous, (hm) half-moon-shaped, (ho) homogeneous, (is) isobilateral, (ly) *S. lycocarpum*, (mu) multicellular, (ol) oblique, (ov) oval, (pl) *S. palinacanthum*, (pn) *S. paniculatum*, (pi) pinnatifid, (pn) pinnately veined, (po) polyhedral, (si) simple, (sm) smooth, (st) *S. stipulaceum*, (ta) tabular, (un) unicellular, (wh) whole, (0) absent, (1) moderate, (2) pronounced.

Table 6
Histochemical leaf features of *Solanum agrarium* Sendtn., *Solanum lycocarpum* A. St.-Hil., *Solanum palinacanthum* Dunal, *Solanum paniculatum* L., and *Solanum stipulaceum* Roem. & Schult.

	Test	Intervein region					Median vein				
		ag	ly	pl	pn	st	ag	ly	pl	pn	st
Primary metabolites											
Starch	Lugol	0	0	1	1	0	0	0	1	1	0
Acidic polysaccharides	Tannic acid	1	1	1	1	1	1	1	1	1	1
	Ruthenium red	1	1	1	1	1	1	1	1	1	1
Proteins	XP	0	1	0	0	1	0	0	1	1	1
	Coomassie blue	0	1	0	0	1	0	1	1	1	1
General lipid	Sudan VI	1	1	1	1	1	1	1	1	1	1
	Sudan black	1	1	1	1	1	1	1	1	1	1
Neutral lipids	Nile blue	1	1	1	1	1	1	1	1	1	1
Acids lipids		1	1	1	1	1	1	1	1	1	1
Secondary metabolites											
Terpenoids	NADI	1	1	1	1	1	1	1	1	1	1
Alcaloids	Ellram	2	2	2	2	2	1	1	1	1	1
	Dittmar	2	2	2	2	2	1	1	1	1	1
Phenolic compounds	Dichromate	2	2	2	2	2	1	1	1	1	1
Tannins	Vanillin	2	2	2	2	2	1	1	1	1	1
Flavonoids	DMACA	2	2	2	2	2	1	1	1	1	1

(ag) *S. agrarium*, (ly) *S. lycocarpum*, (pl) *S. palinacanthum*, (pn) *S. paniculatum*, (st) *S. stipulaceum*, (0) absent, (1) moderate, (2) pronounced.

Chalk, 1957). A wide variation of sieve tube elements and pores diameters was observed, and indicates that these features can be reliably used to distinguish species of this genus. A wide variation of the characteristics of these conducting cells, including the inclination and number of sieve areas, has been reported for the genus *Solanum* (Chavan et al., 2000). Species presenting sieve tubes of large diameter and especially wide pores can benefit from higher nutrient flow rates into developing organs (Mullendore et al., 2010).

The foliar features presented in this study are useful for diagnostic purposes, especially the epidermal features which are well preserved in the raw material. The types of trichomes and stomata, and outline of cell walls are well described on *Solanum* (Araújo et al., 2010; Nurit-Silva et al., 2012; Sampaio et al., 2014). The leaves are widely used as drugs, and are desirable to replace stem and root barks per leaves, because the harvest of barks is damaging for the individual.

The fruits of all the studied species were berries which is in accordance with previous reports for *Solanum* species (Feliciano and Salimena, 2011), and the presence of calcium oxalate crystals, and voluminous intercellular spaces were related by Chiarini and Barboza (2009). Very thick walls, rich in acids and basic polysaccharides, as observed for *S. lycocarpum* mesocarp, constitute water and nutrient reserve mechanisms (Neves et al., 2013).

Analyzing the data obtained for *S. stipulaceum*, some features in particular, such as the absence of spiniform trichomes, presence of stipules, sclerification of the vascular system and medulla of the stem primary structure, and pronounced accumulation of terpenoids in almost all organs, indicate its larger structural difference from the remaining studied species. In fact, according to recent

Table 7
Structural features of pericarps of *Solanum agrarium* Sendtn., *Solanum lycocarpum* A. St.-Hil., *Solanum palinacanthum* Dunal, *Solanum paniculatum* L., and *Solanum stipulaceum* Roem. & Schult.

Features	*Solanum* species				
	ag	ly	pl	pn	st
Morphology					
Type of fruit	be	be	be	be	be
Aroma	0	2	0	0	0
Exocarp					
Color	pu	gr	yl	gr	gr
Consistency	1	2	2	1	2
Mesocarp					
Color	yl	yl	wh	gr	gr
Thickness	1	2	1	1	1
Anatomy					
Exocarp					
Cuticle					
Undulation	2	1	2	1	1
Thickness	1	2	1	1	2
Epidermis					
Cell shape	po	ab	ab	ab	po
Single crystals	0	0	1	0	0
Collenchyma	1	2	1	0	1
Mesocarp					
Cell shape	gl	po	wh	wh	t
Wall thickening	1	2	1	1	2
Intercellular spaces	1	1	2	1	1

(ag) *S. agrarium*, (ab) amoeboid, (be) berry, (br) brachiform, (gl) globoid, (gr) green, (ly) *S. lycocarpum*, (po) polyhedral, (pl) *S. palinacanthum*, (pn) *S. paniculatum*, (pu) purple, (ta) tabular, (st) *S. stipulaceum*, (wh) white, (ye) yellow, (0) absent, (1) moderate, (2) pronounced.

Table 8
Histochemical features of pericarps of *Solanum agrarium* Sendtn., *Solanum lycocarpum* A. St.-Hil., *Solanum palinacanthum* Dunal, *Solanum paniculatum* L., and *Solanum stipulaceum* Roem. & Schult.

	Test	Exocarp					Mesocarp				
		ag	ly	pl	pn	st	ag	ly	pl	pn	st
Primary metabolites											
Starch	Lugol	1	0	0	0	1	1	1	1	1	1
Acidic polysaccharides	Tannic acid	1	1	1	1	1	1	1	1	1	1
	Rhutenium red	1	1	1	1	1	1	1	1	1	1
Proteins	XP	1	1	1	1	1	1	1	1	1	1
	Coomassie blue	1	1	1	1	1	1	1	1	1	1
General lipids	Sudan VI	1	1	1	1	1	1	1	1	1	1
	Sudan black	1	1	1	1	1	1	1	1	1	1
Neutral lipids	Nile blue	1	1	1	1	1	1	0	1	1	1
Acids lipids		0	1	1	0	1	0	1	0	0	1
Secondary metabolites											
Terpenoids	NADI	1	1	1	1	1	1	1	1	1	1
Alcaloids	Ellram	1	1	1	1	1	1	1	1	1	1
	Dittmar	1	1	1	1	1	1	1	1	1	1
Phenolic compounds	Dichromate	1	1	1	1	1	1	1	1	1	1
	Ferric chloride	1	1	1	1	1	1	1	1	1	1
Tanniss	Vanillin	1	1	1	1	1	1	1	1	1	1
Flavonoids	DMACA	1	1	1	1	1	1	1	1	1	1

(ag) *S. agrarium*, (ly) *S. lycocarpum*, (pl) *S. palinacanthum*, (pn) *S. paniculatum*, (st) *S. stipulaceum*, (0) absent, (1) moderate, (2) pronounced.

taxonomy revisions, *S. agrarium, S. lycocarpum, S. palinacanthum, and S. paniculatum* are included in the subgenus *Leptostemonum* (Dunal) Bitter (Levin et al., 2006), whereas *S. stipulaceum* is included in the subgenus *Brevantherum* Seithe (Roe, 1972; Bohs, 2005).

Some anatomical features can reveal the species adaptation mechanisms for these habitats. Aspects of leaf anatomy are informative of the environment where the individuals live (Rossatto and Kolbm, 2012). The presence of tector and glandular trichomes with a variety of shapes has been reported for *Solanum* (Nurit-Silva et al., 2011). A high density of both types of trichomes indicated adaptation to high light, low water availability, and high herbivory rate, typical of the Cerrado. The same occurred for the hypodermis observed in all studied species, which constitutes an additional xeromorphic feature (Rossatto and Kolbm, 2012). The presence of isobilateral mesophyll in *S. lycocarpum* has been previously reported for *Solanum* species growing in habitats with high light but is not in accordance with the dorsiventral mesophyll usually observed for this family (Metcalfe and Chalk, 1957). Strong sclerification was observed in *S. lycocarpum*. Sclerophylly results in the increase of mechanical resistance, as an adaptation to environmental stresses. High levels of sclerophylly can be induced by low water availability, high light intensity, and low concentration of macronutrients, which are common conditions in the Cerrado (Costa et al., 2012; Rossatto and Kolbm, 2012).

S. agrarium is the only annual species of the five studied species. The presence of loose parenchyma at the roots may be related to its short life cycle, which occurs during the short rainfall period that occurs in the Cerrado, when the soil presents high water saturation. Voluminous intercellular spaces favor aeration in organs developing in water saturated soils (Somavilla and Graciano-Ribeiro, 2012). Decreased intercellular spaces minimize excessive water loss, which is relevant in species growing under the predominantly dry Cerrado climate conditions (Milaneze-Gutierre et al., 2003). The investment in starch and protein reserves at the root and stem may be associated with the fact that this species is annual, with the need for fast metabolism due to the emission of a large number of sprouts in a short period of time during the rainy season (Nurit-Silva et al., 2011).

The presence of crystal sand is a unifying feature of the genus *Solanum* (Metcalfe and Chalk, 1957), remaining identifiable even in calcined materials (Furr and Malhberg, 1981). Calcium oxalate crystals are synthesized from endogenous oxalic acid and calcium originating from the environment (Franceschi and Nakata, 2005). In addition to accumulating at the vacuoles, they can be found at the apoplast, in ducts resulting from lysis of crystal idioblasts (Liang et al., 2006). The main function of their formation, especially in developing tissues, seems to be the regulation of calcium concentration, which is needed for the expansion of cells undergoing division (Franceschi and Nakata, 2005; Paiva and Machado, 2005). They can also be involved in protection against herbivores and aluminum detoxification (Nakata, 2003), which are characteristic of the Cerrado biome. The development of crystal ducts from breaking idioblasts, which have cell walls composed mainly of pectin, in recently formed phloem cells close to the cambium layer, was observed in the present study was not related before for the genus.

The medicinal properties mentioned for the species may be associated with the distribution of secondary compounds in the different organs. Histochemical techniques are fast and cheap methods that can be used to identify bioactive classes of compounds in tissues, and cell compartments (Coelho et al., 2012; Demarco et al., 2013; Bedetti et al., 2014). The location of compounds of interest facilitates studies of domestication or obtainment of active principles through biotechnology because it allows the identification of target compartments for plant improvement. The interpretation of histochemical results allows us to compare organs, species, or materials originating from different environments or seasons (Coelho et al., 2012; Adams et al., 2013). Previous histochemical screening can minimize the search for interesting compounds in related plant species, resulting in decreased costs for pharmaceutical research (Saslis-Lagoudakisa et al., 2012).

The anti-inflammatory action attributed to *S. agrarium* (Agra et al., 2007) may be related to the accumulation of the flavonoid kaempferol (Silva et al., 2004), which possesses anti-inflammatory properties (García-Mediavilla et al., 2007). The fruit powder of *S. lycocarpum*, rich in carbohydrates (Rocha et al., 2012), is known for its hypoglycemic properties. The accumulation of alkaloids at the pericarp cells also seems to be related to the traditional use of this species for the control of diabetes (Farina et al., 2010) because glycoalkaloids inhibit the increase of blood glucose (Yoshikawa et al., 2007). Alkaloids are precursors in the synthesis of corticosteroid drugs (Goswami et al., 2003), which may be related to the recommendation of this species as anti-inflammatory (Vieira et al., 2003) and may be linked to terpene chains of hypoglycemic steroid glycoalkaloids (Yoshikawa et al., 2007). The alkaloid chlorogenic

acid inhibits maltase activity in *S. palinacanthum*, decreasing the release of glucose into the blood (Pereira et al., 2008; Kumar et al., 2011). This indicates a possible use of this species for the control of diabetes, which has not been traditionally explored. Rutin, a flavonoid with anti-microbial action, has been isolated from its leaves (Pereira et al., 2008). The accumulation of flavonoids in *S. paniculatum* seems to be related to its antioxidant action (Ribeiro et al., 2007). The hypotensive action of *S. stipulaceum* may be related to the presence of terpenoids, saponins, and alkaloids (Ribeiro et al., 2002).

Conclusions

The identification of structural diagnostic features and classes of chemical compounds with known biological activity present in different organs of the studied species increases the reliability of preparations of pharmaceutical formulations, and reveals a vast area of research in the chemical characterization of molecules related to their traditional medicinal use. Studies relating the structural features with the environmental pressure on the medicinal species, and studies to test the popularly believed properties of native medicinal plants strengthen initiatives to preserve the environments where those species occur naturally, many of them already strongly menaced even before their potential to humankind is known.

Authors' contributions

LJM, ACS, and JMSF contributed in collecting the plant samples, running the laboratory work, and analysis of the data. MOMS, VAR, and LMR designed the study and supervised the laboratory work. All the authors have contributed in drafted the paper, critical reading, writing of the manuscript, and approved the submission.

Ethical disclosures

Protection of human and animal subjects. The authors declare that no experiments were performed on humans or animals for this study.

Confidentiality of data. The authors declare that no patient data appear in this article.

Right to privacy and informed consent. The authors declare that no patient data appear in this article.

Conflicts of interest

The authors declare no conflicts of interest.

Acknowledgments

The authors wish to thank the FAPEMIG for the Research and Technological Development Incentive Scholarship to M.O. Mercadante-Simões (CRA-BIPID-00152-12) and L.M. Ribeiro (CRA-BIPIT-00137-11); the CNPq and FINEP for the Industrial Technology Development scholarship to L.J. Matias (DTI-III-381914/2012-7); the Research Pro-Rectory of the State University of Montes Claros for the Scientific Initiation Scholarship to Ariadna Conceição dos Santos; and Waldimar Ferreira Ruas for collecting the plant material.

References

Adams, S.J., Kuruvilla, G.R., Krishnamurthy, K.V., Nagarajan, M., Venkatasubramanian, P., 2013. Pharmacognostic and phytochemical studies on Ayurvedic drugs Ativisha and Musta. Rev. Bras. Farmacogn. 23, 398–409.
Agra, M.F., Baracho, G.S., Basílio, I.J.D., Nurit, K., Coelho, V.P., Barbosa, D.A., 2007. Sinopse da flora medicinal do Cariri paraibano. Oecol. Bras. 11, 323–330.
Araújo, N.D., Coelho, V.P.M., Agra, M.F., 2010. The pharmacobotanical comparative study of leaves of *Solanum crinitum* Lam., *Solanum gomphodes* Dunal and *Solanum lycocarpum* A. St-Hil (Solanaceae). Rev. Bras. Farmacogn. 20, 666–674.
Araújo, N., Coelho, V.P.M., Ventrella, M.C., Agra, M.F., 2014. Leaf anatomy and histochemistry of three species of *Ficus* sect. *Americanae* supported by light and electron microscopy. Microsc. Microanal. 20, 296–304.
Argyropoulou, C., Akoumianaki-Ioannidou, A., Christodoulakis, N.S., Fasseas, C., 2010. Leaf anatomy and histochemistry of *Lippia citriodora* (Verbenaceae). Aust. J. Bot. 58, 398–409.
Bedetti, C.S., Modolo, L.V., Isaias, R.M.S., 2014. The role of phenolics in the control of auxin in galls of *Piptadenia gonoacantha* (Mart.) MacBr (Fabaceae: Mimosoideae). Biochem. Syst. Ecol. 55, 53–59.
Bohs, L., 2005. Major clades in *Solanum* based in *ndhF* sequences. In: Keating, R.C., Hollowwell, V.C., Croat, T.B. (org.). A festschrift for William G. D'Arcy: The Legacy of a Taxonomist. Monographs in Systematic Botany from the Missouri Botanical Garden. Missouri Botanical Garden Press, St. Louis, pp. 27–49.
Cain, A.J., 1947. The use of Nile Blue in the examination of lipoids. Q. J. Microsc. Sci. 88, 383–392.
Castro, J.A., Brasileiro, B.P., Lyra, D.H., Pereira, D.A., Chaves, J.J., Amaral, C.L.F., 2011. Ethnobotanical study of traditional uses of medicinal plants: the flora of caatinga in the community of Cravolândia-BA, Brazil. J. Med. Plant Res. 5, 1905–1917.
Chavan, R.R., Braggins, J.E., Harris, P.J., 2000. Companion cells in the secondary phloem of Indian dicotyledonous species: a quantitative study. New Phytol. 146, 107–118.
Chiarini, F.E., Barboza, G.E., 2009. Fruit anatomy of species of *Solanum* sect. *Acanthophora* (Solanaceae). Flora 204, 146–156.
Coelho, V.P.M., Leite, J.P.V., Nunes, L.G., Ventrella, M.C., 2012. Anatomy, histochemistry and phytochemical profile of leaf and stem bark of *Bathysa cuspidata* (Rubiaceae). Aust. J. Bot. 60, 49–60.
Costa, V.P., Hayashi, A.H., Carvalho, M.A.M., Silva, E.A., 2012. Aspectos fisiológicos anatômicos e ultra-estruturais do rizoma de *Costus arabicus* L. (Costaceae) sob condições de déficit hídrico. Hoehnea 39, 125–137.
David, R., Carde, J.P., 1964. Coloration différentielle des inclusions lipidique et terpéniques des pseudophylles du *Pin maritime* au moyen du reactif Nadi. C. R. H. Acad. Sci. Paris 258, 1338–1340.
Demarco., D., Castro, M.M., Ascensão, L., 2013. Two laticifer systems in *Sapium haematospermum* – new records for Euphorbiaceae. Botany 91, 545–554.
Endringer, D.C., Valadares, Y.M., Campana, P.R.V., Campos, J.J., Guimarães, K.G., Pezzuto, J.M., Braga, F.C., 2010. Evaluation of Brazilian plants on cancer chemoprevention targets *in vitro*. Phytother. Res. 24, 928–933.
Fahn, A., 1990. Plant Anatomy. Butterworth-Heinemann Ltd, Oxford.
Farina, F., Piassi, F.G., Moysés, M.R., Bazzolli, D.M.S., Bissoli, N.S., 2010. Glycemic and urinary volume responses in diabetic mellitus rats treated with *Solanum lycocarpum*. Appl. Physiol. Nutr. Metab. 35, 40–44.
Feliciano, E.A., Salimena, F.R.G., 2011. Solanaceae in the Serra Negra, Rio Preto, Minas Gerais. Rodriguésia 62, 55–76.
Ferreira, P.R.F., Mendes, C.S.O., Reis, S.B., Rodrigues, C.G., Oliveira, D.A., Mercadante-Simões, M.O., 2011. Morphoanatomy, histochemistry and phytochemistry of *Psidium guineense* Sw. (Myrtaceae) leaves. J. Pharm. Res. 4, 942–944.
Feucht, W., Schmid, P.P.S., Christ, E., 1986. Distribution of flavonols in meristematic and mature tissues of *Prunus avium* shoots. J. Plant Physiol. 125, 1–8.
Fisher, D.B., 1968. Protein staining of ribboned epon sections for light microscopy. Histochemie 16, 92–96.
Franceschi, V.R., Nakata, P.A., 2005. Calcium oxalate in plants: formation and function. Ann. Rev. Plant Biol. 56, 41–71.
Furr, M., Malhberg, P.G., 1981. Histochemical analyses of laticifers and glandular trichomes in *Cannabis sativa*. J. Nat. Prod. 44, 53–159.
Gabe, M., 1968. Techniques histologiques. Masson and Cie, Paris.
García-Mediavilla, V., Crespo, I., Collado, P.S., Esteller, A., Sánchez-Campos, S., Tuñón, M.J., González-Gallego, J., 2007. The anti-inflammatory flavones quercetin and kaempferol cause inhibition of inducible nitric oxide synthase cyclooxygenase-2 and reactive C-protein, and down-regulation of the nuclear factor kappaB pathway in Chang liver cells. Eur. J. Pharmacol. 557, 221–229.
Goswami, A., Kotoky, R., Rastogi, R.C., Ghosh, A.C., 2003. A one-pot efficient process for 16-dehydropregnenolone acetate. Org. Proc. Res. Dev. 7, 306–308.
Jensen, W.A., 1962. Botanical Histochemistry: Principles and Practices. W.H. Freeman and Company, San Francisco.
Johansen, D.A., 1940. Plant Microtechnique. McGraw-Hill Book, New York.
Junikka, L., 1994. Survey of English macroscopic bark terminology. IAWA J. 15, 3–45.
Karnovsky, M.J., 1965. A formaldehyde–glutaraldehyde fixative of high osmolality for use in electron microscopy. J. Cell Biol. 27, 137–138.
Kumar, S., Narwal, S., Kumar, V., Prakash, O., 2011. α-Glucosidase inhibitors from plants: a natural approach to treat diabetes. Pharmacogn. Rev. 5, 19–29.
Levin, R.A., Myers, N.R., Bohs, L., 2006. Phylogenetic relationships among the "spiny solanums" (*Solanum* subgenus *Leptostemonum*, Solanaceae). Am. J. Bot. 93, 157–169.
Liang, S.J., Wu, H., Lun, X., Lu, D.W., 2006. Secretory cavity development and its relationship with the accumulation of essential oil in fruits of

Citrus medica L. var. *sarcodactylis* (Noot.) Swingle. J. Integr. Plant Biol. 48, 573–583.
Mace, M.E., Howell, C.R., 1974. Histochemistry and identification of condensed tannin precursor in roots of cotton seedlings. Can. J. Bot. 52, 2423–2426.
Metcalfe, C.R., Chalk, L., 1957. Anatomy of the Dicotyledons. Oxford University Press, Oxford.
Mercadante-Simões, M.O., Mazzottini-Dos-Santos, H.C., Nery, L.A., Ferreira, P.R.B., Ribeiro, L.M., Royo, V.A., Oliveira, D.A., 2014. Structure, histochemistry and phytochemical profile of the sobol and aerial stem of *Tontelea micrantha* (Celastraceae – Hippocrateoideae). An. Acad. Bras. Cienc. 83, 1167–1179.
Milaneze-Gutierre, M.A., Mello, J.C.P., Delaporte, R.H., 2003. Efeito da intensidade luminosa sobre a morfo-anatomia foliar de *Bouchea fluminensis* (Vell) Mold. (Verbenaceae) e sua importância no controle de qualidade da droga vegetal. Rev. Bras. Farmacogn. 13, 23–33.
Moreira, A.S.F., Lemos Filho, J.P., Isaias, R.M.S., 2013. Structural adaptations of two sympatric epiphytic orchids (Orchidaceae) to a cloudy forest environment in rocky outcrops of Southeast Brazil. Rev. Biol. Trop. 61, 1053–1065.
Mullendore, D.L., Windt, C.W., Van As, H., Knoblauch, M., 2010. Sieve tube geometry in relation to phloem flow. Plant Cell 22, 579–593.
Nakata, P.A., 2003. Advances in our understanding of calcium oxalate crystal formation and function in plants. Plant Sci. 164, 901–909.
Neves, S.C., Ribeiro, L.M., Cunha, I.R.G., Pimenta, M.A.S., Mercadante-Simões, M.O., Lopes, P.S.N., 2013. Diaspore structure and germination ecophysiology of the babassu palm (*Attalea vitrivir*). Flora 208, 68–78.
Nurit-Silva, K., Costa-Silva, R., Coelho, V.P.M., Agra, M.F., 2011. Pharmacobotanical study of vegetative organs of *Solanum torvum* Kiriaki. Rev. Bras. Farmacogn. 21, 568–574.
Nurit-Silva, K., Costa-Silva, R., Basílio, I.J.L.D., Agra, M.F., 2012. Leaf epidermal characters of Brazilian species of *Solanum* section *Torva* as taxonomic evidence. Can. J. Microbiol. 58, 806–814.
O'Brien, T.P., Feder, N., Mccully, M.E., 1964. Polychromatic staining of plant cell walls by toluidine blue O. Protoplasma 59, 368–373.
Paiva, E.A.S., Machado, S.R., 2005. Role of intermediary cells in *Peltodon radicans* (Lamiaceae) in the transfer of calcium and formation of calcium oxalate crystals. Braz. Arch. Biol. Technol. 48, 147–153.
Paiva, E.A.S., Pinho, S.Z., Oliveira, D.M.T., 2011. Large plant samples: how to process for GMA embedding? In: Chiarini-Garcia, H., Melo, R.C.N. (orgs.). Light Microscopy: Methods and Protocols. Springer Humana Press, New York, pp. 37–49.
Pearse, A.G.E., 1980. Histochemistry Theoretical and Applied. Churchill Livingston, Edinburgh.
Pereira, A.C., Oliveira, D.F., Silva, G.H., Figueiredo, H.C.P., Cavalheiro, A.J., Carvalho, D.A., Souza, L.P., Chalfoun, S.M., 2008. Identification of the antimicrobial substances produced by *Solanum palinacanthum* (Solanaceae). An. Acad. Bras. Cienc. 80, 427–432.
Picoli, E.A.T., Isaias, R.M.S., Ventrella, M.C., Miranda, R.M., 2013. Anatomy, histochemistry and micromorphology of leaves of *Solanum granuloso-leprosum* Dunal. Biosci. J. 29, 655–666.
Pizzolato, T.D., Lillie, R.D., 1973. Mayer's tannic acid-ferric chloride stain for mucins. J. Histochem. Cytochem. 21, 56–64.
Ribeiro, E.A.N., Batitucci, M.C.P., Lima, J.A.T., Araújo, I.A.G., Mauad, H., Medeiros, I.A., 2002. Cardiovascular effects induced by the aqueous fraction of the ethanol extract of the stem of *Solanum stipulaceum* in rats. Rev. Bras. Farmacogn. 12, 34–35.
Ribeiro, S.R., Fortes, C.C., Oliveira, S.C.C., Castro, C.F.S., 2007. Avaliação da atividade antioxidante de *Solanum paniculatum* (Solanaceae). A. Cien. S. Univ. Paran. 11, 179–183.
Rocha, D.A., Abreu, C.M.P., Sousa, R.V., Corrêa, A.D., 2012. Método de obtenção e análise da composição centesimal do polvilho da fruta-de-lobo (*Solanum lycocarpum* St. Hil). Rev. Bras. Frut. 34, 248–254.
Roe, K.E., 1972. A revision of *Solanum* section *Brevantherum* (Solanaceae). Brittonia 24, 239–278.
Rossatto, D.R., Kolbm, R.M., 2012. Structural and functional leaf traits of two *Gochnatia* species from distinct growth forms in a sclerophyll forest site in Southeastern Brazil. Acta Bot. Bras. 26, 849–856.
Sampaio, V.S., Araújo, N.D., Agra, M.F., 2014. Characters of leaf epidermis in *Solanum* (clade Brevantherum) species from Atlantic forest of Northeastern Brazil. S. Afr. J. Bot. 94, 108–113.
Santos, A.V., Defavieri, A.C.V., Bizzo, H.R., Gil, R.A.S.S., Sato, A., 2013. *In vitro* propagation, histochemistry, and analysis of essential oil from conventionally propagated and in vitro-propagated plants of *Varronia curassavica* Jacq. In Vitro Cell Dev. Biol. Plant 49, 405–413.
Saslis-Lagoudakisa, C.H., Savolainen, V., Williamsond, E.M., Forestc, F., Wagstaffe, S.J., Baralf, S.R., Watsong, M.F., Pendryg, C.A., Hawkinsa, J.A., 2012. Phylogenies reveal predictive power of traditional medicine in bioprospecting. Proc. Natl. Acad. Sci. U. S. A. 25, 15835–15840.
Silva, T.M.S., Nascimento, R.J.B., Câmara, C.A., Castro, R.N., Braz-Filho, R., Agra, M.F., Carvalho, M.G., 2004. Distribution of flavonoids and N-transcaffeoyltyramine in *Solanum* subg. *Leptostemonum*. Biochem. Syst. Ecol. 32, 513–516.
Somavilla, N.S., Graciano-Ribeiro, D., 2012. Ontogeny and characterization of aerenchymatous tissues of Melastomataceae in the flooded and well-drained soils of a Neotropical savanna. Flora 207, 212–222.
Stehmann, J.R., Mentz, L.A., Agra, M.F., Vignoli-Silva, M., Giacomin, L., Rodrigues, I.M.C., 2014. Solanaceae. Lista de Espécies da Flora do Brasil. Jardim Botânico do Rio de Janeiro, Available from: http://floradobrasil.jbrj.gov.br/jabot/floradobrasil/FB14716 (accessed 19.10.15).
Svendsen, A.B., Verpoorte, R., 1983. Chromatography of Alkaloids. Elsevier Scientific Publishing Company, New York.
Vidal, B.C., 1970. Dichroism in collagen bundles stained with xylidine-Ponceau 2R. Ann. Histochem. 15, 289–296.
Vieira Jr., G., Ferreira, P.M., Matos, L.G., Ferreira, E.C., Rodovalho, W., Ferri, P.H., Ferreira, H.D., Costa, E.A., 2003. Anti-inflammatory effect of *Solanum lycocarpum* fruits. Phytother. Res. 17, 892–896.
World Health Organization, 2013. WHO Traditional Medicine Strategy 2014–2023. WHO Library Cataloguing-in-Publication Data, Geneva.
Yoshikawa, M., Nakamura, S., Ozaki, K., Kumahara, A., Morikawa, T., Matsuda, H., 2007. Structures of steroidal alkaloid oligoglycosides, robeneosides A and B, and antidiabetogenic constituents from the Brazilian medicinal plant *Solanum lycocarpum*. J. Nat. Prod. 70, 210–214.